

# The Super-Strong Coupling Regime of Cavity Quantum Electrodynamics

D. Meiser and P. Meystre

*Department of Physics, The University of Arizona, 1118 East 4th Street, Tucson, AZ 85721*

We describe a qualitatively new regime of cavity quantum electrodynamics, the super strong coupling regime. This regime is characterized by atom-field coupling strengths of the order of the free spectral range of the cavity, resulting in a significant change in the spatial mode functions of the light field. It can be reached in practice for cold atoms trapped in an optical dipole potential inside the resonator. We present a nonperturbative scheme that allows us to calculate the frequencies and linewidths of the modified field modes, thereby providing a good starting point for a quantization of the theory.

PACS numbers: 42.50.Fx,42.50.Pq,42.50-p

A striking characteristic of cavity quantum electrodynamics (CQED) is the conceptual simplicity of the systems involved. Typically, photons in a single cavity mode interact with atoms with a very small relevant number of internal quantum states [1]. On the experimental side this simplicity leads to the precise control of most system parameters and to the laboratory realization of many idealized theoretical models and Gedankenexperiments. For example, strongly nonclassical states of the light field such as e.g. number states [2, 3] can be created, the entanglement between light and atoms can be studied, and important questions related to the quantum measurement process can be addressed. Over the last two decades experimentalists further expanded the scope of CQED by achieving increasing control over the translational degrees of freedom of the atoms via laser cooling and other cooling schemes, and CQED also plays an important role in quantum information research.

In the *strong coupling regime* of CQED the coherent interaction between a single atom and the light field, characterized by the Rabi frequency  $\Omega_R$ , dominates over the decoherence processes induced by the coupling to the environment, and characterized by the spontaneous decay rate  $\gamma$  and the cavity damping rate  $\kappa$ ,

$$\Omega_R > \gamma, \kappa. \quad (1)$$

In contrast to these three characteristic frequencies, whose relative role in CQED has been explored in great detail in the past, the role of the free spectral range  $\omega_{\text{FSR}}$  of the resonator has largely been ignored so far. However, if one can achieve experimental conditions such that

$$\Omega_R > \omega_{\text{FSR}} \quad (2)$$

the coupled atoms-cavity system enters a qualitatively new regime which we refer to as the *super-strong coupling regime*.

The reason why that regime has not been clearly identified in the past is that  $\omega_{\text{FSR}} = c/2L \sim Q\gamma$ , where  $L$  is the resonator length and  $Q$  its quality factor, is under most circumstances much too large to lead to significant effects. Loosely speaking, the strong coupling regime is reached by making the photons pass through and interact with the atoms many times by employing high-Q resonators whereas for the super-strong coupling regime the

interaction has to be significant already in one cavity round-trip. As we show in this letter, this regime is now within experimental reach for ultracold atoms trapped in an optical lattice inside an optical resonator [4]. In this setting, in contrast to the single atom case of conventional CQED, one uses the cooperative back-action of many atoms on the light field to obtain sufficiently strong coupling.

A hallmark of the super-strong coupling regime is that the resonator modes are significantly modified from their vacuum form. This can be seen by considering the first-order correction to an unperturbed mode function,

$$\varphi_n^{(1)}(z) = \varphi_n^{(0)}(z) + \sum_{m \neq n} \frac{\langle \varphi_m^{(0)} | \hat{V} | \varphi_n^{(0)} \rangle}{\omega_n - \omega_m} \varphi_m^{(0)}(z), \quad (3)$$

where the interaction Hamiltonian  $\hat{V}$  accounts for the atoms-field interaction,  $|\varphi_m^{(0)}\rangle$  is the unperturbed cavity mode of frequency  $\omega_m$  and  $\varphi_m^{(i)}(z) = \langle z | \varphi_m^{(i)} \rangle$  is the wavefunction for the  $i$ -th order of the perturbation series. Since the energy separations in the denominator in Eq. (3) are of the order of the free spectral range  $\omega_{\text{FSR}}$  and  $\langle \varphi_m^{(0)} | \hat{V} | \varphi_n^{(0)} \rangle$  is of the order of  $\Omega_R$ , it follows that in the super-strong coupling regime every mode acquires an admixture of the unperturbed cavity modes – or in extreme cases a perturbative description may even become meaningless.

We consider the specific situation where  $N$  two-level atoms with transition frequency  $\omega_a$  are trapped by an optical dipole potential inside a Fabry-Pérot resonator with mirror reflectivities  $R_1$  and  $R_2$  and mirror separation  $L$ , see Fig. 1. The  $z$ -direction is chosen as the optical axis. Two phase-locked laser beams with frequency  $\omega$  and amplitudes  $E_l$  and  $E_r$  are injected through the left and right mirror, respectively. We assume that the light is far detuned from the atomic transition frequency,  $|\Delta| = |\omega - \omega_a| \gg \gamma, \Omega_R$ , so that the excited atomic state can safely be adiabatically eliminated. Furthermore, if both the transverse beam profile  $u_\perp(r, \varphi; z)$  and the transverse atomic density profile  $\rho_\perp(r, \varphi; z)$  vary slowly with  $z$ , the transverse dimensions can be integrated out, as discussed e.g. in [5], resulting in a one-dimensional effective model.

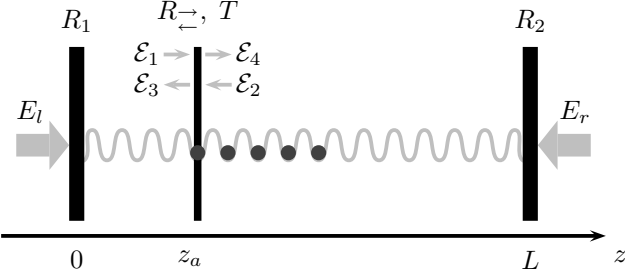


Figure 1: Schematic of atoms trapped in an optical lattice potential in a cavity. Also shown are the effective mirror at  $z_a$  representing the atoms and the boundary conditions for the incoming and outgoing fields at this mirror.

In this limit the one-dimensional optical dipole potential is

$$V_{\text{dipole}}(z) = g(z)|E(z)|^2 \quad (4)$$

where

$$g(z) = \frac{2\phi^2}{\hbar\Delta} A(z), \quad (5)$$

and  $A(z) = \int_0^\infty dr \int_0^{2\pi} d\varphi |u_\perp(r, \varphi; z)|^2 \rho_\perp(r, \varphi; z)$  is a measure of the overlap between the atomic density profile and the beam profile and is slowly varying with  $z$ . The potential Eq. (4) describes an optical lattice whose spacing must be determined self-consistently such that the atoms at each lattice site are at a local potential minimum. With the lattice spacing determined this way the light field scattered off the atoms at every site interferes constructively in the *backwards* direction, see Ref. [6]. In this sense the lattice automatically fulfills a somewhat generalized Bragg condition corresponding to maximal reflection regardless of possibly inhomogeneous occupation numbers at the individual lattice sites. We therefore assume for simplicity a uniform filling of  $N_s$  sites with  $n$  atoms each.

If the local width of the atomic density distribution in the  $z$ -direction is much smaller than an optical wavelength, which is typically the case, we can approximate it as

$$\rho(z) = \sum_{l=0}^{N_s-1} n\delta(z - z_a - ld), \quad (6)$$

where  $z_a$  is the position of the first occupied lattice site and

$$d = \frac{\pi + 2 \arctan \Lambda}{k} \quad (7)$$

is the lattice period. Here  $k = \omega/c$  is the wave vector of the light and

$$\Lambda = \frac{gnk}{4\epsilon_0} \quad (8)$$

is a dimensionless parameter characterizing the interaction between light and atoms at a single lattice site.

Our starting point for the non-perturbative determination of the cavity modes is the classical one-dimensional propagation equation

$$\frac{\partial^2 E(z)}{\partial z^2} + k^2 E(z) = \frac{g}{2} k^2 \rho(z) E(z). \quad (9)$$

which can be easily obtained by inserting the polarization in the far detuned limit,  $P(z, t) = -\frac{g}{2\epsilon_0} \rho(z) E(z, t)$ , into the Maxwell equations and by using that the atomic density distribution changes very little during one round trip of the light in the cavity,  $\omega_{\text{FSR}}^{-1}$ .

The problem is greatly simplified by replacing the atomic density distribution Eq. (6) by an effective mirror at a location  $z_a$  to be determined later on, with reflection coefficients  $R_→$  and  $R_←$  for the right- and left-propagating fields and a transmission coefficient  $T$ , see Fig. 1. This is possible since the Maxwell wave equation for the light is linear once the density distribution is fixed.

For the particular density distribution (6) the total reflection and transmission coefficients are readily found by the transfer matrix method as [5, 6, 7],

$$R_→ = \frac{-i\Lambda N e^{-2i \arctan \Lambda}}{1 - i\Lambda N} \quad (10)$$

$$R_← = \frac{-i\Lambda N e^{-2i \arctan \Lambda (2N-1)}}{1 - i\Lambda N} \quad (11)$$

$$T = \frac{e^{-2i \arctan \Lambda N}}{1 - i\Lambda N}. \quad (12)$$

The steady-state boundary conditions

$$\mathcal{E}_1 = T_1 e^{ikz_a} E_l + e^{2ikz_a} R_1 \mathcal{E}_2, \quad (13)$$

$$\mathcal{E}_2 = R_→ \mathcal{E}_1 + T \mathcal{E}_3, \quad (14)$$

$$\mathcal{E}_3 = R_2 e^{2ik(L-z_a)} \mathcal{E}_4 + T_2 e^{ik(L-z_a)} E_r, \quad (15)$$

$$\mathcal{E}_4 = T \mathcal{E}_1 + R_← \mathcal{E}_3, \quad (16)$$

are then easily solved for the field amplitudes at the effective mirror, see Fig. 1, where  $\mathcal{E}_1$  and  $\mathcal{E}_3$  correspond to the field amplitudes to the left of the first atom and the amplitudes at every other atom are easily found using again the transfer matrix method. From these amplitudes the field can be determined anywhere inside the cavity through free space propagation.

In our specific example the mode functions are substantially altered provided that the reflection coefficient  $|R_→|^2 = |R_←|^2$  is of order unity, which is equivalent to  $N\Lambda \sim 1$ , see Eq. (10). There are many possible ways to achieve such a large value. For example, in the case of  $^{87}\text{Rb}$  atoms radially localized much more tightly than the optical beam waist of  $30 \cdot 10^{-6}$  mm,  $\varphi = 2.32 \cdot 10^{-29}$  Cm,  $\lambda \simeq 800$  nm, a detuning  $\Delta = -10^9 \text{s}^{-1}$ , we have that  $A \approx 3.5 \cdot 10^8 \text{m}^{-2}$  and  $\Lambda/n \approx -9 \cdot 10^{-7}$ . For a total number of Rb atoms of  $10^6$  we then find  $|R|^2 \approx 0.45$ . All figures in this letter are for these parameters, together with cavity

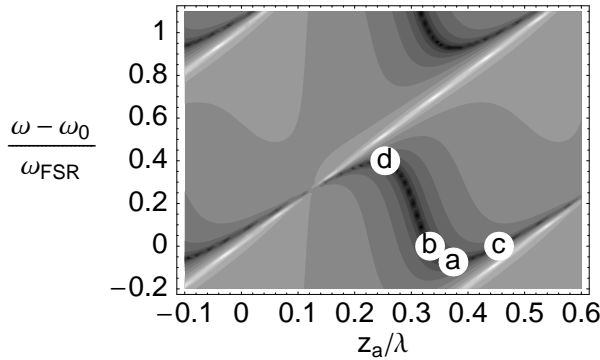


Figure 2: Logarithmic plot of the optical dipole potential for the collective motion of the atoms, for the parameters of the text. The darker shades correspond to the potential minima. Here and in Fig. 4 the points (a-d) label the positions at which the envelopes in Fig. 3 are calculated and we have chosen the offset frequency  $\omega_0 = 10^4 \omega_{\text{FSR}}$ .

mirror reflection coefficients of  $|R_1|^2 = |R_2|^2 = 0.99$  and  $E_r \equiv 0$ . Note that for the case of atoms in an optical lattice the deviation of  $T$  from unity is of the same order in the interaction as the reflection coefficients. Thus it is a peculiarity of that case that it is in general inconsistent to keep the phase shifts the light suffers upon transmission through the atomic cloud while at the same time neglecting the reflection coefficients. Finally, we note that appreciable reflection coefficients have been demonstrated in an experiment by Slama et. al. [7] in which reflection coefficients of atoms in an optical lattice as high as 30% were demonstrated, albeit with resonant light.

The mode functions are fully determined once the atomic position  $z_a$  is fixed by the altered, self-consistent optical dipole potential. Figure 2 shows the potential felt by the atoms at the leftmost lattice site. The potentials at the other sites are very similar. The dipole potential is periodic along the  $z_a$  axis with period  $\lambda/2$ , and along the  $\omega$  axis with period  $\omega_{\text{FSR}}$ . Its distortion due to the back-action of the atoms on the optical field is clearly evident, and the resulting bistability of the atomic position has been discussed in Ref. [5].

In the following we assume that the atoms are always located in a local potential minimum. With the atomic positions fixed in this manner we then study the intra-cavity field envelopes as a function of the frequency of the incident fields. Figure 3 shows the envelopes of the electromagnetic field determined for the points (a) through (d) of Fig. 2. In this example,  $10^6$  atoms are distributed over 1000 lattice sites so that the optical lattice is approximately 500 optical wavelengths long. It is apparent from the figure that the envelope strongly depends on the frequency of the incident light and the atomic position. Point (a) is at the low frequency edge of the resonance region, just below the branching point of the dipole potential. At this point the field amplitudes at the two

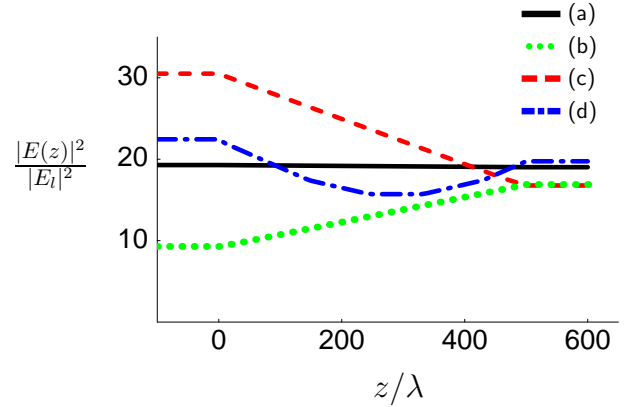


Figure 3: (Color online) Field envelopes across the optical lattice for (a)  $\omega = -0.074 \omega_{\text{FSR}}$ , (b) and (c)  $\omega = 0$  and (d)  $\omega = 0.39 \omega_{\text{FSR}}$  and the respective atomic positions as shown in Fig. 2 and 4. For parameters see text.

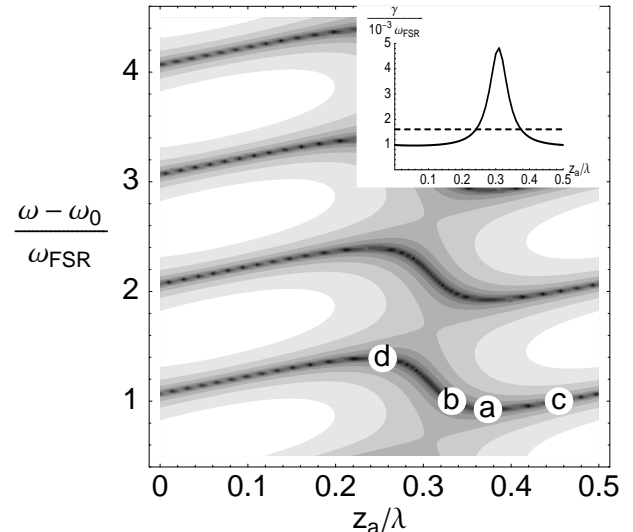


Figure 4: Logarithmic plot of  $|D(\omega)|^{-2}$  for the parameters of the text, with the dark regions corresponding to very small  $D$  and signifying resonant behavior. The inset shows the linewidth  $\Gamma$  as a function of  $z_a$ , with the reflection coefficients of the atoms taken into account (solid line) and neglected (dashed line).

edges of the optical lattice are exactly  $\pi$  out of phase (for an odd number of lattice sites the fields would be exactly in phase with the same implications) and the field penetrates the optical lattice almost unperturbed, just as it would in free space [6]. Above the branching point the field looks entirely different depending on the local minimum in which the atoms are situated. In the left valley the field is stronger to the left of the atoms and in the right valley it is stronger on the right. Near the point where the two local minima merge again (modulo  $\lambda/2$ ) the electrical field amplitude is extremely sensitive to the frequency of the incident field as the left and right dominated modes “collide” at this point.

The solutions for the field amplitudes are linear combinations of the injected fields  $E_l$  and  $E_r$ , with coefficients having resonant denominators given by the determinant of the set of Eqs. (16),

$$D(k) = 1 - R_2 R_{\leftarrow} e^{2ik(L-z_a)} - R_1 R_{\rightarrow} e^{2ikz_a} - R_1 R_2 (T^2 - R_{\rightarrow} R_{\leftarrow}) e^{2ikL}. \quad (17)$$

The position  $\omega_0$  and width  $\Gamma$  of the resonances of the optical cavity dressed by the trapped atoms are given by the complex zeros  $k_0$  of that determinant.

Figure 4, which shows  $1/|D(k)|^2$  as a function of  $z_a$ , illustrates these dressed resonances. For each atomic position  $z_a$  there is an infinite series of such resonances, separated by the free spectral range  $\omega_{\text{FSR}}$ . The resonance frequencies depend on the atomic positions, and their distortion compared to the case of an empty resonator can be of the order of  $\omega_{\text{FSR}}$ , confirming that that system is in the super-strong coupling regime. Furthermore, as can be seen in the inset in Fig. 4, the position of the atoms also affects the width of the resonances, even in the absence of additional losses due to spontaneous emission from the atoms, as is the case in our example. The resonance can even become narrower than for the empty cavity, making it very clear that an interpretation of the linewidth changes in terms of additional loss channels is impossible. The changes in resonance width are however naturally expected for the three mirror cavity suggested in Fig. 1, see e.g. [8]. The influence of the atoms on the resonator linewidth is in contrast to the conventional situation in CQED, which is recovered by setting  $R_{\rightarrow} = R_{\leftarrow} = 0$  and normalizing  $T$  to unity for lossless atoms in Eq. (17). The determinant reduces then to  $D_{R=0}(k) = 1 - R_1 R_2 e^{2i(kL+\phi)}$ , where  $\phi$  is the phase of  $T$ . From this expression it is clear that in that limit the interaction with the atoms can only lead to shifts of the resonance frequencies but not to a change in the linewidths, see the inset in Fig. 4. Also, all changes in the spectral properties are now independent of the atomic position  $z_a$ .

The classical theory discussed in this letter offers a good basis for the quantization of the cavity field: One can introduce field operators for the self-consistent modes determined from the boundary conditions (16), with frequencies given by the zeros of the determinant (17). The

modified linewidths shown in the insert of Fig. 4 find their physical origin in the change in the overlap between the cavity field and the continuum of modes outside the resonator, and can therefore be modelled using standard quantum optics methods such as e.g. a Born-Markov master equation.

Quantization along these lines is obviously only possible if the atoms are in a state with an exact  $R$  as opposed to a superposition of several  $R$ . Unpublished calculations indicate that this is given, for  $d$  as in Eq. (7), if the total number of atoms is fixed. Currently we investigate the more general case that presents substantial new difficulties.

It is important to keep in mind that in this system the boundary conditions are dynamical since the atomic reflection and transmission coefficients, as well as  $z_a$ , typically change in time. As a result, the resonance frequency and the linewidth also change over time. In general, the quantization of the electromagnetic field with time-dependent boundary conditions is a difficult problem, see e.g. [9]. In the present case, we note that since the spatial mode structure is established over a time scale of the order of the round-trip time  $1/\omega_{\text{FSR}}$ , one must have

$$\frac{d|R|^2}{dt}, \frac{d|T|^2}{dt}, \frac{d(z_a/\lambda)}{dt} \ll \omega_{\text{FSR}} \quad (18)$$

for the above quantization procedure to work. If these conditions are not satisfied a single-mode theory becomes inadequate and one must resort to a full multimode description.

In addition to addressing the problem of quantization in detail, future work will investigate modifications in the cooling of the atomic motion through the inclusion of the atomic reflection coefficient and study the various aspects of problems concerning spontaneous symmetry breaking and phase transitions in the classical and quantum cases by exploiting the bistability of the optical dipole potential.

This work is supported in part by the US Office of Naval Research, by the National Science Foundation, by the US Army Research Office, by the Joint Services Optics Program, and by the National Aeronautics and Space Administration.

---

[1] Good starting points to access the wealth of publications on the subject are: P. R. Berman, *Cavity quantum electrodynamics*, Academic Press (1994); S. Haroche in *New Trends in Atomic Physics*, Les Houches, Session XXXVIII, Ed. by G. Grynberg and R. Stora, Elsevier Science Pubs. B. V. (1982); P. Meystre, “Cavity quantum optics and the quantum measurement process”, in *Progress in Optics Vol. 30*, Ed. E. Wolf, Elsevier (1992).

[2] J. Krause, M. O. Scully, T. Walther, and H. Walther, Phys. Rev. A **39**, 1915 (1989).

[3] S. Brattke, B. T. H. Varcoe, and H. Walther, Phys. Rev. Lett. **86**, 3534 (2001).

[4] M. Greiner, O. Mandel, T. Esslinger, T. W. Hänsch, and I. Bloch, Nature (London) **415**, 39 (2002).

[5] D. Meiser and P. Meystre, Phys. Rev. A **73**, 033417 (2006).

[6] I. H. Deutsch, R. J. C. Spreeuw, S. L. Rolston, and W. D. Phillips, Phys. Rev. A **52**, 1394 (1995).

[7] S. Slama, C. von Cube, M. Kohler, C. Zimmermann, and P. W. Courteille, Phys. Rev. A **73**, 023424 (2006).

[8] R. Dändliker and T. Tschudi, Appl. Opt. **8**, 1119 (1969).

[9] C. K. Law, Phys. Rev. A **51**, 2537 (1995).